HHS Public Access

Author manuscript

Acad Radiol. Author manuscript; available in PMC 2017 October 01.

Published in final edited form as:

Acad Radiol. 2016 October ; 23(10): 1255–1263. doi:10.1016/j.acra.2016.02.002.

CT-derived Biomechanical Metrics Improve Agreement Between Spirometry and Emphysema

Surya P. Bhatt, M.D.[*,1,2], **Sandeep Bodduluri, M.S.**[*,3], **John D. Newell Jr., M.D.**[3], **Eric A. Hoffman, Ph.D.**[3], **Jessica C. Sieren, Ph.D.**[3], **Meilan K. Han, M.D., M.S.**[4], **Mark T. Dransfield, M.D.**[1,2], and **Joseph M. Reinhardt, Ph.D.**[3] **for the COPDGene Investigators**

[1]Division of Pulmonary, Allergy and Critical Care Medicine, University of Alabama at Birmingham, Birmingham, AL 35294

[2]UAB Lung Health Center, University of Alabama at Birmingham, Birmingham, AL 35294

[3]Department of Radiology and Biomedical Engineering, University of Iowa, Iowa City, IA 52242

[4]Division of Pulmonary & Critical Care Medicine, University of Michigan, Ann Arbor, MI 48109

Abstract

Rationale and Objectives—Many COPD patients have marked discordance between FEV_1 and degree of emphysema on CT. Biomechanical differences between these patients have not been studied. We aimed to identify reasons for the discordance between CT and spirometry in some patients with COPD.

Materials and Methods—Subjects with GOLD stage I–IV from a large multicenter study (COPDGene) were arranged by percentiles of %predicted FEV_1 and emphysema on CT. Three categories were created using differences in percentiles: Cat_{spir} with predominant airflow obstruction/minimal emphysema, Cat_{CT} with predominant emphysema/minimal airflow obstruction, and $Cat_{matched}$ with matched FEV_1 and emphysema. Image registration was used to derive Jacobian determinants, a measure of lung elasticity, anisotropy and strain tensors, to assess biomechanical differences between groups. Regression models were created with the above categories as outcome variable, adjusting for demographics, scanner type, quantitative CT-derived emphysema, gas trapping, and airway thickness (Model 1), and after adding biomechanical CT metrics (Model 2).

Corresponding author: Surya P. Bhatt, M.D., University of Alabama at Birmingham, Division of Pulmonary, Allergy and Critical Care Medicine, THT 422, 1720, 2nd Avenue South, Birmingham, AL 35294 spbhatt@uab.edu.

*Co first authors

Author Contributions:

Study design: SPB, SB, JDN, EAH and JMR

Statistical analyses: SB and SPB

Data interpretation: SPB, SB, MKH, JDN, JCS, MTD, EAH and JMR

Manuscript writing: SPB, SB, EAH and JMR

Critical review of the manuscript for important intellectual content: SPB, SB, MKH, JDN, JCS, MTD, EAH and JMR

SPB is the guarantor of the content of the manuscript, including the data and analysis.

Clinical Trial Registration: ClinicalTrials.gov NCT00608764

Results—Jacobian determinants, anisotropy and strain tensors were strongly associated with FEV_1. With $Cat_{matched}$ as control, Model 2 predicted Cat_{spir} and Cat_{CT} better than Model 1 (Akaike Information Criterion, AIC 255.8 vs. 320.8). In addition to demographics, the strongest independent predictors of FEV_1 were Jacobian mean (β= 1.60,95%CI = 1.16 to 1.98; p<0.001), coefficient of variation (CV) of Jacobian (β= 1.45,95%CI = 0.86 to 2.03; p<0.001) and CV strain (β= 1.82,95%CI = 0.68 to 2.95; p = 0.001). CVs of Jacobian and strain are both potential markers of biomechanical lung heterogeneity.

Conclusions—CT-derived measures of lung mechanics improve the link between quantitative CT and spirometry, offering the potential for new insights into the linkage between regional parenchymal destruction and global decrement in lung function in COPD patients.

Keywords

Emphysema; spirometry; COPD; discordance

Introduction

The diagnosis of chronic obstructive pulmonary disease (COPD) is currently based on the detection of airflow obstruction by spirometry.[1] It is increasingly recognized that airflow obstruction as measured by impairment in the forced expiratory volume in 1 second (FEV_1) does not fully explain the morbidity associated with the disease, and this functional definition can be complemented by anatomic measures of disease using widely available imaging modalities.[2] Computed tomography (CT) has become the gold standard in the quantitative assessment of the presence and distribution of emphysema, a major component of COPD, and relies on using a fixed Hounsfield threshold value below which all lung areas are deemed emphysematous in a CT scan obtained at full inspiration.[3] CT measures of emphysema correlate well with pathology,[4] and numerous studies have shown a strong correlation between spirometry and CT emphysema. [5–12] The agreement between CT emphysema and spirometry is however not perfect, and in some cases, CT densitometry may be more sensitive in detecting emphysema than spirometry.[6,13]

It is our observation that many COPD patients have marked discordance between FEV_1 and degree of emphysema on volumetric CT.[14,15] Some subjects with severe airflow obstruction have mild emphysema on CT and conversely, some patients with severe emphysematous destruction of the lung have relatively mild spirometric impairment. While some of these differences, especially in the former group, are likely due to airway narrowing, the reasons for this discrepancy between expected changes on spirometry and CT have not been systematically studied, particularly in the disproportionate emphysema group. Since airflow obstruction is due to a combination of airway narrowing and loss of elastic recoil due to emphysema, it is possible that static single-volume CT images do not capture lung mechanics sufficiently to explain lung function defects. We hypothesized that biomechanical measures of regional lung tissue expansion and contraction using image registration applied to paired inspiratory and expiratory CT scans will provide a link between CT-derived quantitative measures and spirometry. Through a demonstration of this link, we seek to provide an improved understanding of patient specific links between the presence and distribution of quantitative emphysema and airflow obstruction.

Materials and Methods

Data Collection

Data for this study was acquired from the Genetic Epidemiology of COPD (COPDGene) study; this is a large multicenter study of current and former smokers aged 45 to 80 years. Details of the study protocol have been previously published.[16] Post bronchodilator spirometry was performed using the ndd Easy-One spirometer to assess airflow obstruction.[17] COPD was diagnosed based on a fixed threshold for the ratio of FEV_1 to the forced vital capacity (FVC) of <0.70; disease severity was graded according to the Global initiative for chronic Obstructive Lung Disease (GOLD) guidelines.[1] Reference values for spirometry were drawn from the National Health and Nutrition Examination Survey (NHANES) III cohort.[18] Volumetric CT scans were acquired with the subject in supine position during a carefully coached breath hold to either full inspiration (total lung capacity, TLC) or end tidal expiration (functional residual capacity, FRC); or at one center to full expiration (residual volume, RV).[16] The scans followed an imaging protocol with collimation, 0–5mm; tube voltage, 120kV; tube current 200mAs; gantry rotation time of 0.5s; and pitch, 1.1. The images were reconstructed with a standard kernel with a slice thickness of 0.75 mm and a reconstruction interval of 0.5 mm. 3D Slicer software (www.airwayinspector.org) was used to measure emphysema and gas trapping. Pulmonary Workstation 2 (VIDA Diagnostics, Coralville, IA, USA) was used to measure airway dimensions. [16]. Emphysema was quantified by using the percentage of voxels at TLC with attenuation less than −950 Hounsfield Units (HU) (low attenuation area, $\%LAA950_{insp}$), and also as the HU value at the 15th percentile (Perc15). [16,19] Gas trapping was calculated as the percentage of voxels at FRC with attenuation less than −856 HU ($\%LAA856_{exp}$).[20] We used wall area percentage of segmental airways (WA%) and gas trapping to measure airway disease.[16] The COPDGene study was approved by the institutional review boards of all 21 participating centers, and written informed consent was obtained from each subject.

Case Selection

Subjects with GOLD stage I to IV disease, without physician-diagnosed bronchial asthma and with good quality expiratory images, were included. As there is no published data on the degree of emphysema to be expected for a given value of FEV_1, we used the percentile method to assess discrepancy between CT and spirometry to derive a sample size of convenience and also to create two widely disparate groups by spirometry and CT emphysema. In addition, as we have previously demonstrated strong independent correlations between CT emphysema, gas trapping and Jacobian metrics with airflow obstruction on spirometry, we did not analyze all subjects in the cohort as adding biomechanical metrics to measurements of lung disease with such strong correlations is not expected to provide additional explanations of mechanics, especially in subjects who are highly concordant for CT and spirometry and constitute the majority of subjects.[14,21] In order to study those who have significant discordance in the severity of CT and spirometric findings, we used the percentile method to express differences and discordance. We arranged all subjects (n=2982) in ascending order of severity of airflow obstruction as assessed by percent predicted FEV_1 to calculate the percentile values for spirometric abnormality; a second list was created by arranging all subjects in ascending order of severity of CT

emphysema as determined by the continuous measure Perc15 percentile. Concordance between spirometry and CT was assessed by subtracting percentile ranking for CT from percentile ranking for spirometry. Those with values closest to 0 (n=100) were considered "Matched" as they had expected ranking for spirometry compared to CT emphysema, and this group served as the reference group. Those with the greatest positive percentile ranking difference for spirometry compared to CT (n=100) were considered spirometry predominant, and those with the greatest positive percentile ranking difference for CT compared to spirometry (n=100) were considered CT predominant. 3 subjects in the CT predominant group were excluded due to failure of image registration matching.

Image Registration

The inspiratory and expiratory CT images were registered for each subject, and expiratory image matched to inspiratory image. Details of image registration are provided in the Supplement. Briefly, a non-rigid lung mass-preserving registration method was used to capture volume changes between these two targeted lung inflation levels.[21,22] A sum of squared tissue volume difference was used as a similarity metric. This similarity criterion aims to find a registration transformation that minimizes the local difference of tissue volume inside the lungs scanned at different pressure levels. This method has been shown to be effective in lung image registration protocols.[21–23] The final transformation matrix from inspiration to expiration was derived from the registration protocol and in turn used to extract displacement field information.

Three measures were calculated from the registration process: Jacobian, strain information, and anisotropic deformation index (ADI). *Jacobian* measures the local volume change and estimates the pointwise volume expansion and contraction during the deformation from inspiration to expiration. Jacobian has values from 0 to infinity. A Jacobian value of 1 indicates neither local expansion nor contraction. Values greater than or lesser than 1 represent local expansion and contraction respectively. Maximum principle *strain* was computed from the displacement field information to extract how much a given displacement differs locally from inspiration to expiration. Strain analysis expresses the geometric deformation caused by action of stress in the lung. *ADI* provides the orientation preference of lung deformation by calculating the ratio of length in the direction of maximal extension to the length in the direction of minimal extension within a unit volume of 1 mm.[23] The larger the ADI value, more the anisotropy is with deformation. The coefficient of variation (CV) across the whole lung was calculated for each of these biomechanical measures to assess heterogeneity and dispersion.

Statistical Analyses

Univariate regression analyses were performed for CT variables with FEV_1 to assess association, and those with $p<0.05$ were included in multivariable models. Multivariable analyses were also adjusted for clinically important variables including age, sex, race, body mass index (BMI) and scanner type. Multicollinearity diagnostics were performed and variables with a variance inflation factor of greater than 10 (strain mean, ADI mean and ADI CV) were excluded from the model. Independent contribution of each covariate to the variance in FEV_1 was calculated using squared semi-partial correlation coefficient (r^2).

Further, to assess differences in the discordant groups of interest, three categories were created using differences in percentile rankings: Cat_{spir} with predominant airflow obstruction on spirometry and minimal CT emphysema; Cat_{CT} with predominant CT emphysema and relatively minimal airflow obstruction on spirometry; and $Cat_{matched}$ with matched FEV_1 and CT emphysema. Two regression models were created with mentioned categories as outcome variables using multinomial logistic regression. CT variables significantly associated with FEV_1 were entered into the models and all models were adjusted for age, race, sex, BMI, and CT scanner type. At this stage, $\%LAA950_{insp}$ was substituted for Perc15 as a measure of emphysema as Perc15 was already used to derive the groups, and $\%LAA950_{insp}$ is more commonly used clinically to quantify CT emphysema. Model A comprised of $\%LAA950_{insp}$, $\%LAA856_{exp}$ and WA%. Biomechanical measures (mean Jacobian, CV of Jacobian, and CV of strain) were added to the predictors in Model A to create Model B. With $Cat_{matched}$ as reference category, multinomial logistic regression was used to predict Cat_{spir} and Cat_{CT}. Model fit statistics are shown in terms of Akaike Information Criterion (AIC) derived from information theory. AIC is used to estimate the quality and model comparisons and is defined as: AIC = −2Lm+ 2k, where Lm represents maximum log-likelihood and K is the number of variables in the model. AIC takes both goodness of fit and number of variables into account while penalizing the increase in number of variables and thus avoids over fitting scenarios. The smaller the AIC, the better is the model prediction. All analyses were performed using R statistical software (Version 3.0.1) and Statistical Package for the Social Sciences (SPSS 22.0, SPSS Inc., Chicago, IL, USA).

Results

The three categories were well separated by percentile differences for spirometry and CT emphysema. The percentile difference in the Cat_{spir} category was −65.7 (SD8.2), range −93.5 to −53.2; difference in Cat_{CT} was 61.1 (7.8), range 51.6 to 79.1; and in $Cat_{matched}$ was −0.04 (0.63), range −1.03 to 1.06 ($p<0.001$ for all comparisons). Representative cases are depicted in Figure 1. Baseline demographics, spirometry and CT features for the three categories are described in Table 1. Compared to those in the $Cat_{matched}$, those with Cat_{spir} were younger and were more obese. There were significant differences in airway disease between the three categories, with the disproportionate spirometric category showing most airway disease.

A number of CT metrics of lung deformation were associated with airflow obstruction. On univariate analyses, there was a significant association between FEV_1 and Jacobian mean (regression coefficient $\beta = 2.49$, 95%CI 2.17 to 2.81; $p<0.001$), Jacobian CV ($\beta = 3.90$, 95%CI 3.38 to 4.42; $p<0.001$), ADI mean ($\beta = 0.25$, 95%CI 0.20 to 0.30; $p<0.001$), ADI CV ($\beta = 0.69$, 95%CI 0.52 to 0.87; $p<0.001$), strain mean ($\beta = 3.55$, 95%CI 3.16 to 3.94; $p<0.001$) and strain CV ($\beta = -1.68$, 95%CI −3.06 to −0.30; $p = 0.017$). Of these, after assessment of multicollinearity, Jacobian mean, Jacobian CV and strain CV were selected for inclusion in the multivariable model to predict independent associations with FEV_1 (Table 2). We also assessed the relative independent contributions of the CT metrics and found that the Jacobian mean explained 5.6% of the variation in FEV_1 compared to CT emphysema which explained only 2.8%. Wall area% and Jacobian CV were other strong

predictors, explaining 3.9% and 2.3% of the variance in FEV_1, respectively (Supplemental Table 1).

Table 3 shows a comparison of measures of lung mechanics between the three categories. The same measures of lung mechanics that were significant on univariate regression with FEV_1, and after collinearity adjustments were included in the two multinomial logistic regression models shown in Table 4. Comparison of AIC between the two models shows that inclusion of biomechanical measures (Model 2) predicts the categories better than the model that contains only static single-volume based CT metrics of structural lung disease (Model 1), AIC 255.8 vs. 320.8. As worsening disease can result in increase in TLC, which in turn can compensate for increase in RV and tend to preserve FVC and thus FEV_1, we also performed sensitivity analyses with addition of CT measured TLC to the above model, with no change in prediction of FEV_1 (data not shown).

Discussion

We show that using dual-volume based biomechanical measures of lung tissue deformation rather than static single-volume measures of CT emphysema considerably improves prediction of spirometric airflow obstruction and also concordance between CT and spirometry. This improved linkage between CT metrics and spirometry provides a validation of the mechanics-based measures derived from image matching, and offers the ability to link regional lung mechanics to spirometry which provides only a single metric reflecting a composite of regional lung differences. By providing a comprehensive map of regional lung mechanics coupled with regional maps of emphysema, patient selection for therapies for severe emphysema can be better determined and outcomes can be evaluated in light of this new understanding of lung structure-function relationships.

A number of studies have analyzed the correlation between static single-volume CT measures of emphysema and spirometric airflow obstruction. One large study examining this showed a correlation between the two of −0.76 when emphysema was defined at <−950HU threshold.[24] While this degree of correlation is good, it leaves room for a significant amount of discrepancy. Emphysema is a heterogeneous disease and the distribution of lung disease affects spirometry. Studies that examined the relative distribution of emphysema by zone found that upper zone emphysema correlates better with the diffusing capacity of carbon monoxide whereas predominant lower zone emphysema correlates better with FEV_1. [25–28] We previously showed that emphysema like changes in the right middle lobe correlate the least with spirometry.[29] There is also a differential effect of central versus peripheral involvement of the lung, with a greater correlation of central involvement with FEV_1.[25] However, these studies do not provide a composite measure of emphysema that improves agreement with spirometry. While CT gas trapping as an indirect measure of small airway disease has a greater correlation with airflow obstruction,[14] this is likely significantly influenced by the degree of baseline emphysema in the preceding respiratory cycles.[30]

We add to the literature by showing three additional measures that improve agreement between CT and spirometry. Not surprisingly, the spirometry predominant group had significantly greater airway disease. Perhaps of more interest is the CT predominant group in

which subjects had substantial degrees of emphysema with relatively minimal airflow obstruction. The divergence in emphysema measures and expected spirometry impairment is likely partly due to the fact that single-volume-based CT measures are static whereas spirometry is a dynamic measure. By using image registration applied to matched pairs of inspiratory-expiratory CT scans, we show an improved agreement between dynamic spirometric measures and biomechanical CT measures. While measures of airways disease including differences in airway wall thickness and air trapping also account for some of the disagreement, we found that after adjustment for indices of airway disease, biomechanical measures account for considerable additional variability. Our findings suggest that the presence of CT emphysema may not always translate into airflow obstruction, and that not all emphysema translates into loss of elastic recoil equally. The image-matching-based metrics more directly link CT-based findings with the integrated mechanics associated with spirometry.

We found that a greater value for the Jacobian mean predicts a higher FEV_1. The Jacobian mean is reflective of the over-all volume change of the individual lung regions. Ju et al showed that greater degree of lobar heterogeneity of emphysema on single-volume CT images was associated with less airflow obstruction.[31] We extend these findings by demonstrating that image-matching based measures of biomechanical heterogeneity (Jacobian and strain CVs) are predictive of lung function, and these biomechanical changes are provided on a lobar and sub-lobar basis. It is pertinent to note that the Jacobian CV and strain CV are more strongly associated with the prediction of the Cat_{CT} category, one in which there is significant CT emphysema but the spirometric abnormality remains relatively masked. Though we did not assess the type of emphysema qualitatively, panlobular emphysema tends to be more homogeneous, is associated with higher lung compliance, and is associated with a lower FEV_1 for the same level of quantitative emphysema of centrilobular distribution.[32,33] Centrilobular emphysema tends to be more heterogeneous and is associated with lesser FEV_1 reduction for a given degree of emphysema. This is especially relevant for subjects with very mild airflow obstruction who might harbor significant structural lung disease prior to development of spirometric abnormality. We speculate that more local heterogeneity indicates relative canceling effects of the pressure effects created by greater and lesser expansive lung regions, a form of local pseudorestriction. The Jacobian CV might be a novel measure of biomechanical lung heterogeneity that can explain a significant proportion of the discrepancy. We acknowledge that some of the biomechanical measures that have significant associations with outcome categories have wide confidence intervals, perhaps reflecting the relatively small sample size of subjects included in the analysis.

Our findings have a number of potential clinical implications. The diagnosis of COPD has traditionally relied on demonstrating airflow obstruction on spirometry. CT emphysema has been proposed as a new metric of disease that provides complementary information but it has been observed that the amount of CT-based emphysema does not directly translate to the degree of airflow obstruction.[34] By providing CT-derived measures of regional lung mechanics to the more commonly used quantitative CT metrics derived from a single lung volume, we now provide a closer link between quantitative CT and spirometry. Further research is needed to find out whether these metrics can aid earlier diagnosis of disease

before the onset of airflow obstruction which is a global measure of lung disease. CT emphysema is used for assessment of structural lung disease and assessing regional heterogeneity of emphysema for interventions such as bronchoscopic lung volume reduction. Patient selection might be better served by the inclusion of regional measures of lung mechanics to the list of measures assessed by quantitative CT. Addition of biomechanical measures prior to lung resection surgeries may also improve prediction of postoperative lung function.

Our study has some limitations. First, CT scans were not spirometrically gated and variations in respiratory effort may affect the reproducibility of Jacobian measures; however, patients were coached to maximum inspiration and end exhalation. Second, this was a multicenter study and hence a number of scanners were used to acquire the CT scans. However, we did adjust for scanner variability in our analyses, and emphysema and air trapping were assessed from the same lung volumes as those used for the biomechanical measures, thus linking these measures to each other, accounting, in part, for protocol differences and subject variability. Third, although we adjusted for airway disease by use of WA%, the current resolution of CT limits visualization of airways beyond the segmental level. There is also a growing understanding that WA% is a composite of changes in airway wall thickness and luminal dimensions and may not fully reflect peripheral airway disease.[35] To address these issues, we also used gas trapping as a surrogate of small airways disease. Fourth, CT scans were obtained at only two volumes, thus limiting our ability to account for regional differences in lung mechanics reflected in the non-linearity of the pressure volume curve either on a global or regional basis.[36] With the considerable reduction in radiation doses afforded by evolving CT detector and x-ray gun technologies coupled with improved iterative reconstruction methods,[37,38] improved details of mechanical characteristics of the lung, by utilizing dynamic imaging or greater numbers of lung volumes, may become more practical while limiting radiation exposure. Finally, even though we reduced the sample size to 300, this was intentionally done to examine the cases with the most discordance. This was necessary as there is no previous literature to guide us as to how much abnormality on CT predicts the abnormality on spirometry and vice versa. Although subjects with no airflow obstruction can have a significant degree of emphysema, we did not include these subjects as they are more likely to have matched CT-Spirometry values than those with disease, and hence would heavily influence our analyses. Our study also has a number of strengths. Sites were continuously coached in regards to the proper performance of lung volume coaching and CT protocol adherence. Study subjects were drawn from a cohort that is well characterized phenotypically, and hence included a large sample size and included a high proportion of African Americans.

In conclusion, compared to single-volume CT assessment of emphysema, biomechanical measures derived from dual-volume CT show improved agreement with airflow obstruction on spirometry. This has implications for disease detection, for the understanding of links between regional lung disease and spirometrically derived lung function, as well as therapy planning.

Supplementary Material

Refer to Web version on PubMed Central for supplementary material.

Acknowledgments

Funding Source:

National Heart, Lung and Blood institute grant numbers: R01 HL089897, R01 HL089856 and R01 HL122438.

References

1. Vestbo J, Hurd SS, Agusti AG, et al. Global strategy for the diagnosis, management, and prevention of chronic obstructive pulmonary disease: GOLD executive summary. Am J Respir Crit Care Med. 2013; 187(4):347–365. [PubMed: 22878278]
2. Coxson HO, Leipsic J, Parraga G, Sin DD. Using pulmonary imaging to move chronic obstructive pulmonary disease beyond FEV1. Am J Respir Crit Care Med. 2014; 190(2):135–144. [PubMed: 24873985]
3. Uppaluri R, Mitsa T, Sonka M, Hoffman EA, McLennan G. Quantification of pulmonary emphysema from lung computed tomography images. Am J Respir Crit Care Med. 1997; 156(1): 248–254. [PubMed: 9230756]
4. Madani A, Zanen J, de Maertelaer V, Gevenois PA. Pulmonary emphysema: objective quantification at multi-detector row CT--comparison with macroscopic and microscopic morphometry. Radiology. 2006; 238(3):1036–1043. [PubMed: 16424242]
5. Heremans A, Verschakelen JA, Van fraeyenhoven L, Demedts M. Measurement of lung density by means of quantitative CT scanning. A study of correlations with pulmonary function tests. Chest. 1992; 102(3):805–811. [PubMed: 1516407]
6. Hesselbacher SE, Ross R, Schabath MB, et al. Cross-sectional analysis of the utility of pulmonary function tests in predicting emphysema in ever-smokers. Int J Environ Res Public Health. 2011; 8(5):1324–1340. [PubMed: 21655122]
7. Kinsella M, Muller NL, Abboud RT, Morrison NJ, DyBuncio A. Quantitation of emphysema by computed tomography using a “density mask” program and correlation with pulmonary function tests. Chest. 1990; 97(2):315–321. [PubMed: 2298057]
8. Haraguchi M, Shimura S, Hida W, Shirato K. Pulmonary function and regional distribution of emphysema as determined by high-resolution computed tomography. Respiration. 1998; 65(2):125–129. [PubMed: 9580924]
9. Gould GA, Redpath AT, Ryan M, et al. Lung CT density correlates with measurements of airflow limitation and the diffusing capacity. Eur Respir J. 1991; 4(2):141–146. [PubMed: 2044729]
10. Washko GR, Criner GJ, Mohsenifar Z, et al. Computed tomographic-based quantification of emphysema and correlation to pulmonary function and mechanics. Copd. 2008; 5(3):177–186. [PubMed: 18568842]
11. Aziz ZA, Wells AU, Desai SR, et al. Functional impairment in emphysema: contribution of airway abnormalities and distribution of parenchymal disease. AJR Am J Roentgenol. 2005; 185(6):1509–1515. [PubMed: 16304005]
12. Pauls S, Gulkin D, Feuerlein S, et al. Assessment of COPD severity by computed tomography: correlation with lung functional testing. Clin Imaging. 2010; 34(3):172–178. [PubMed: 20416480]
13. Spaggiari E, Zompatori M, Verduri A, et al. Early smoking-induced lung lesions in asymptomatic subjects. Correlations between high resolution dynamic CT and pulmonary function testing. Radiol Med. 2005; 109(1–2):27–39. [PubMed: 15729184]
14. Bhatt SP, Sieren JC, Dransfield MT, et al. Comparison of spirometric thresholds in diagnosing smoking-related airflow obstruction. Thorax. 2014; 69(5):409–414. [PubMed: 23525095]
15. Lutchmedial SM, Creed WG, Moore AJ, Walsh RR, Gentchos GE, Kaminsky DA. How Common is Airflow Limitation in Patients with Emphysema on Computerized Tomography of the Chest? Chest. 2014

16. Regan EA, Hokanson JE, Murphy JR, et al. Genetic epidemiology of COPD (COPDGene) study design. Copd. 2010; 7(1):32–43. [PubMed: 20214461]
17. Miller MR, Hankinson J, Brusasco V, et al. Standardisation of spirometry. Eur Respir J. 2005; 26(2):319–338. [PubMed: 16055882]
18. Hankinson JL, Odencrantz JR, Fedan KB. Spirometric reference values from a sample of the general U.S. population. American journal of respiratory and critical care medicine. 1999; 159(1): 179–187. [PubMed: 9872837]
19. Zach JA, Newell JD Jr, Schroeder J, et al. Quantitative computed tomography of the lungs and airways in healthy nonsmoking adults. Investigative radiology. 2012; 47(10):596–602. [PubMed: 22836310]
20. Busacker A, Newell JD Jr, Keefe T, et al. A multivariate analysis of risk factors for the air-trapping asthmatic phenotype as measured by quantitative CT analysis. Chest. 2009; 135(1):48–56. [PubMed: 18689585]
21. Bodduluri S, Newell JD Jr, Hoffman EA, Reinhardt JM. Registration-based lung mechanical analysis of chronic obstructive pulmonary disease (COPD) using a supervised machine learning framework. Acad Radiol. 2013; 20(5):527–536. [PubMed: 23570934]
22. Reinhardt JM, Ding K, Cao K, Christensen GE, Hoffman EA, Bodas SV. Registration-based estimates of local lung tissue expansion compared to xenon CT measures of specific ventilation. Medical image analysis. 2008; 12(6):752–763. [PubMed: 18501665]
23. Amelon R, Cao K, Ding K, Christensen GE, Reinhardt JM, Raghavan ML. Three-dimensional characterization of regional lung deformation. J Biomech. 2011; 44(13):2489–2495. [PubMed: 21802086]
24. Schroeder JD, McKenzie AS, Zach JA, et al. Relationships between airflow obstruction and quantitative CT measurements of emphysema, air trapping, and airways in subjects with and without chronic obstructive pulmonary disease. AJR Am J Roentgenol. 2013; 201(3):W460–470. [PubMed: 23971478]
25. Nakano Y, Sakai H, Muro S, et al. Comparison of low attenuation areas on computed tomographic scans between inner and outer segments of the lung in patients with chronic obstructive pulmonary disease: incidence and contribution to lung function. Thorax. 1999; 54(5):384–389. [PubMed: 10212100]
26. Gurney JW, Jones KK, Robbins RA, et al. Regional distribution of emphysema: correlation of high-resolution CT with pulmonary function tests in unselected smokers. Radiology. 1992; 183(2): 457–463. [PubMed: 1561350]
27. Saitoh T, Koba H, Shijubo N, Tanaka H, Sugaya F. Lobar distribution of emphysema in computed tomographic densitometric analysis. Invest Radiol. 2000; 35(4):235–243. [PubMed: 10764092]
28. Parr DG, Stoel BC, Stolk J, Stockley RA. Pattern of emphysema distribution in alpha1-antitrypsin deficiency influences lung function impairment. Am J Respir Crit Care Med. 2004; 170(11):1172–1178. [PubMed: 15306534]
29. Bhatt SP, Sieren JC, Newell JD Jr, Comellas AP, Hoffman EA. Disproportionate contribution of right middle lobe to emphysema and gas trapping on computed tomography. PLoS One. 2014; 9(7):e102807. [PubMed: 25054539]
30. Han MK. Clinical correlations of computed tomography imaging in chronic obstructive pulmonary disease. Ann Am Thorac Soc. 2013; 10(Suppl):S131–137. [PubMed: 24313763]
31. Ju J, Li R, Gu S, et al. Impact of emphysema heterogeneity on pulmonary function. PLoS One. 2014; 9(11):e113320. [PubMed: 25409328]
32. Kim WD, Eidelman DH, Izquierdo JL, Ghezzo H, Saetta MP, Cosio MG. Centrilobular and panlobular emphysema in smokers. Two distinct morphologic and functional entities. Am Rev Respir Dis. 1991; 144(6):1385–1390. [PubMed: 1741553]
33. Saetta M, Kim WD, Izquierdo JL, Ghezzo H, Cosio MG. Extent of centrilobular and panacinar emphysema in smokers' lungs: pathological and mechanical implications. Eur Respir J. 1994; 7(4):664–671. [PubMed: 8005246]
34. Enright P. HRCT-defined emphysema is not COPD to be treated with inhalers. Thorax. 2014; 69(5):401–402. [PubMed: 24393768]

35. Smith BM, Hoffman EA, Rabinowitz D, et al. Comparison of spatially matched airways reveals thinner airway walls in COPD. The Multi-Ethnic Study of Atherosclerosis (MESA) COPD Study and the Subpopulations and Intermediate Outcomes in COPD Study (SPIROMICS). Thorax. 2014; 69(11):987–996. [PubMed: 24928812]

36. Jahani N, Yin Y, Hoffman EA, Lin CL. Assessment of regional non-linear tissue deformation and air volume change of human lungs via image registration. J Biomech. 2014; 47(7):1626–1633. [PubMed: 24685127]

37. Sieren JP, Hoffman EA, Fuld MK, Chan KS, Guo J, Newell JD Jr. Sinogram Affirmed Iterative Reconstruction (SAFIRE) versus weighted filtered back projection (WFBP) effects on quantitative measure in the COPDGene 2 test object. Med Phys. 2014; 41(9):091910. [PubMed: 25186397]

38. Newell JD Jr, Fuld MK, Allmendinger T, et al. Very low-dose (0.15 mGy) chest CT protocols using the COPDGene 2 test object and a third-generation dual-source CT scanner with corresponding third-generation iterative reconstruction software. Invest Radiol. 2015; 50(1):40–45. [PubMed: 25198834]

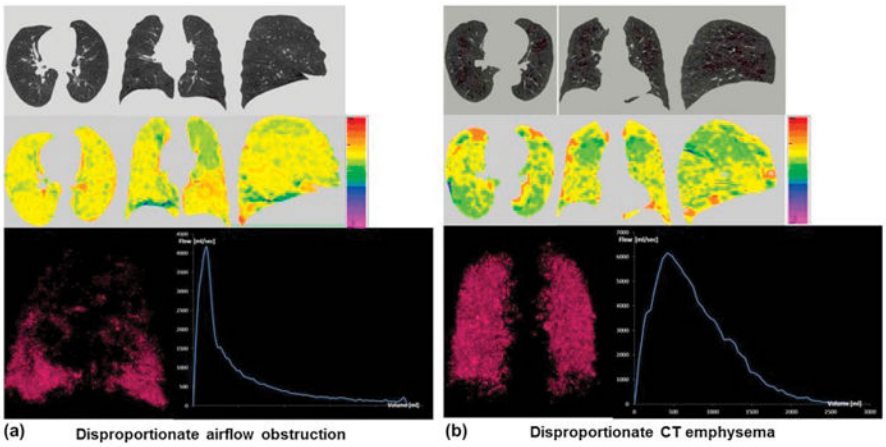

Figure 1.

Panel A shows computed tomographic (CT) images for subject with severe airflow obstruction (FEV_1 %predicted 32.6) but with relatively minimal emphysema (1.5% volume <−950HU on end inspiratory images). **Panel B** shows features for subject with severe emphysema on CT (20.8%) but with relatively minimal airflow obstruction (FEV_1 %predicted 99.6). Top row represents the overlay of emphysema voxels on the CT images. Middle row represents the overlay of Jacobian color map on the CT images from each category. Jacobian value (=1) represents no deformation; >1 represents local expansion; <1 local contraction. Bottom row represents 3D visualization of emphysema voxels in each category with flow volume loop.

Table 1

Demographic information, radiographic and spirometry measures

	Cat_{spir} (n=100)	Cat_{CT} (n=97)	$Cat_{matched}$ (n=100)
Age (years)	60.4 (7.8) **	65.0 (8.2)	64.5 (9.0)
Sex (%Males)	60 (60)	69 (71)	57 (57)
Race (%Non Hispanic Whites)	74 (74) *	85 (88)	84 (84)
BMI (kg/m^2)	33 (7.3) ***	26.6 (5.2)	26.4 (6.0)
Smoking packyears	57.3 (29.0)	51.4 (25.8)	50.4 (24.3)
FEV_1 (L)	1.15 (0.35) **	2.75 (0.68) ¥	1.45 (0.82)
FEV_1 % predicted	38.0 (9.0) ¥	92.6 (13.7) ¥	50.8 (26.6)
FVC (L)	2.29 (0.63) ¥	4.48 (0.94) ¥	3.01 (0.94)
FEV_1/FVC	0.51 (0.10) *	0.61 (0.07) ¥	0.46 (0.17)
%Emphysema (LAA_{insp}<−950 HU)	1.5 (1.2) ¥	17.3 (8.9)	19.4 (18.0)
%Gas trapping (LAA_{exp}<−856 HU)	20.5 (12.6) ¥	34.9 (11.8) **	44.5 (26.4)
Wall Area%	65.1 (2.7) ¥	59.3 (2.4) ¥	62.2 (2.8)

All values expressed as mean (standard deviation) unless other specified.

* p<0.05

** p<0.01

¥ p<0.001

Cat_{spir} = category with disproportionate spirometric abnormality. Cat_{CT} = category with disproportionate CT abnormality. $Cat_{matched}$ = matched CT and spirometric abnormalities. BMI = Body mass index. FEV_1 = Forced expiratory volume in the first second. FVC = Forced vital capacity. LAA_{insp}<−950 HU = Low attenuation areas <−950 Hounsfield Units at end inspiration. LAA_{exp}<−856 HU = Low attenuation areas < −856 Hounsfield Units at end expiration. Wall Area% = (wall area/total bronchial area)×100, calculated as the average of six segmental bronchi in each subject.

Table 2

Univariate and Multivariable linear regression for prediction of FEV_1

	Univariate			Multivariable		
Variable	**Parameter estimate**	**95% CI**	**P value**	**Parameter estimate**	**95% CI**	**p value**
Age (years)	−0.010	−0.022 to 0.003	0.134	−0.19	−0.026 to −0.011	<0.001
Male Sex	−0.69	−0.90 to −0.48	<0.001	−0.53	−0.65 to −0.40	<0.001
LAA_{insp}<−950 HU	−0.010	−0.018 to −0.003	0.007	−0.026	−0.035 to −0.016	<0.001
LAA_{exp}<−856 HU	−0.014	−0.019 to −0.009	<0.001	0.006	0.001 to 0.014	0.115
Wall Area%	−0.21	−0.26 to −0.16	<0.001	−0.07	−0.10 to −0.05	<0.001
Jacobian Mean	2.49	2.17 to 2.81	<0.001	1.60	1.16 to 1.98	<0.001
Jacobian CV	3.90	3.38 to 4.42	<0.001	1.45	0.86 to 2.03	<0.001
Strain CV	−1.68	−3.06 to −0.30	0.017	1.82	0.68 to 2.95	0.001

FEV_1 = Forced expiratory volume in the first second. CI = Confidence intervals. LAA_{insp}<−950 HU = Low attenuation areas <−950 Hounsfield Units at end inspiration. LAA_{exp}<−856 HU = Low attenuation areas <−856 Hounsfield Units at end expiration. Wall Area% = (wall area/total bronchial area)×100, calculated as the average of six segmental bronchi in each subject. CV = Coefficient of variation.

Multivariable model included variables significant on univariate analyses in the Table and were also adjusted for age, body mass index, sex, race and scanner type. R^2 for multivariable model = 0.73

Table 3

Biomechanical CT measures for the three categories

	Cat_{spir} (n=100)	**Cat_{CT} (n=97)**	**$Cat_{matched}$ (n=100)**
Jacobian Mean	1.38 (0.18)	1.73 (0.20)¥	1.44 (0.23)
Jacobian CV	0.21 (0.08)*	0.46 (0.16)¥	0.25 (0.10)
Strain Mean	0.36 (0.12)*	0.65 (0.15)¥	0.41 (0.16)
Strain CV	0.57 (0.07)¥	0.61 (0.06)	0.62 (0.09)
ADI Mean	1.03 (0.53)	3.20 (2.71)¥	1.34 (0.94)
ADI CV	1.06 (0.36)*	1.71 (0.69)¥	1.25 (0.36)

All values expressed as mean (standard deviation) unless other specified.

*$p<0.05$

¥$p<0.001$

CT = computed tomography. Cat_{spir} = category with disproportionate spirometric abnormality. Cat_{CT} = category with disproportionate CT abnormality. $Cat_{matched}$ = matched CT and spirometric abnormalities. CV = Coefficient of variation. ADI = Anistropic deformation index.

Table 4

Multivariable Logistic Regression Models for Predicting Disproportionate Categories

Model 1				
	Cat_{spir}		**Cat_{CT}**	
	Odds Ratio	**95%CI**	**Odds Ratio**	**95%CI**
$LAA<-950_{insp}$	0.40¥	0.25–0.62	0.94	0.91–1.03
$LAA<-856_{exp}$	1.14**	1.06–1.23	1.05*	1.01–1.10
WA%	1.96¥	1.53–2.52	1.47¥	1.24–1.75
Model 2				
	Cat_{spir}		**Cat_{CT}**	
	Odds Ratio	**95%CI**	**Odds Ratio**	**95%CI**
$LAA<-950_{insp}$	0.62*	0.39–0.98	0.96	0.89–1.04
$LAA<-856_{exp}$	0.94	0.84–1.06	0.98	0.92–1.04
WA%	1.63¥	1.22–2.18	1.20	0.98–1.47
Jacobian mean	17.05¥	4.84–60.11	4.38¥	2.15–8.93
Jacobian CV	21.98*	4.47–65.04	5.96¥	2.75–12.9
Strain CV	2.16	0.76–6.15	1.83*	1.01–3.31

Cat_{spir} = category with disproportionate spirometric abnormality. Cat_{CT} = category with disproportionate CT abnormality. $Cat_{matched}$ = matched CT and spirometric abnormalities. LAA_{insp}<−950 HU = Low attenuation areas <−950 Hounsfield Units at end inspiration. LAA_{exp}< −856 HU = Low attenuation areas <−856 Hounsfield Units at end expiration. Wall Area% = (wall area/total bronchial area)×100, calculated as the average of six segmental bronchi in each subject. CV = Coefficient of variation.

All models adjusted for age, race, sex, body mass index and scanner type.

* p<0.05

** p<0.01

¥ p<0.001

R^2 for Model 1 =0. 56. R^2 for Model 2 = 0. 66. AIC for Model 1 = 320.8, AIC for Model 2 = 255.8.